MOLECULAR AND CELLULAR BIOLOGY, Nov. 2003, p. 8233–8245 Vol. 23, No. 22
0270-7306/03/$08.00+0 DOI: 10.1128/MCB.23.22.8233–8245.2003

Neurons Expressing the Highest Levels of γ-Synuclein Are Unaffected by Targeted Inactivation of the Gene

Natalia Ninkina,[1] Katerina Papachroni,[1]† Darren C. Robertson,[1] Oliver Schmidt,[1] Liz Delaney,[1]‡ Francis O'Neill,[1] Felipe Court,[1] Arnon Rosenthal,[2] Susan M. Fleetwood-Walker,[1] Alun M. Davies,[1] and Vladimir L. Buchman[1]*

Department of Preclinical Veterinary Sciences, University of Edinburgh, Edinburgh EH9 1QH, United Kingdom,[1] and Rinat Neuroscience Corporation, Palo Alto, California 94304[2]

Received 9 June 2003/Returned for modification 18 July 2003/Accepted 14 August 2003

Homologous recombination in ES cells was employed to generate mice with targeted deletion of the first three exons of the γ-*synuclein* gene. Complete inactivation of gene expression in null mutant mice was confirmed on the mRNA and protein levels. Null mutant mice are viable, are fertile, and do not display evident phenotypical abnormalities. The effects of γ-synuclein deficiency on motor and peripheral sensory neurons were studied by various methods in vivo and in vitro. These two types of neurons were selected because they both express high levels of γ-synuclein from the early stages of mouse embryonic development but later in the development they display different patterns of intracellular compartmentalization of the protein. We found no difference in the number of neurons between wild-type and null mutant animals in several brain stem motor nuclei, in lumbar dorsal root ganglia, and in the trigeminal ganglion. The survival of γ-synuclein-deficient trigeminal neurons in various culture conditions was not different from that of wild-type neurons. There was no difference in the numbers of myelinated and nonmyelinated fibers in the saphenous nerves of these animals, and sensory reflex thresholds were also intact in γ-synuclein null mutant mice. Nerve injury led to similar changes in sensory function in wild-type and mutant mice. Taken together, our data suggest that like α-synuclein, γ-synuclein is dispensable for the development and function of the nervous system.

Several neurodegenerative diseases have been recently coalesced into a distinct group named synucleinopathies (12, 16, 20, 53). Although they are diverse in symptoms and clinical signs, these diseases share a common histopathological feature, i.e., formation of large intracellular inclusions whose principal component is an aggregated small protein, α-synuclein. Neither the normal cellular function of α-synuclein nor the exact mechanism of its involvement in neurodegeneration is clearly understood; possible scenarios are discussed in many recent reviews (see, for example, references 10, 28, 33, 34, and 43). Even less clear are the normal functions and roles in neurodegeneration of the other two members of the synuclein family. Both β-synuclein/PNP14 (24, 35) and γ-synuclein/BCSG1/persyn (7, 26, 29) have a very high degree of amino acid similarity with α-synuclein within the N-terminal KTK repeat region of the protein molecule, and this is reflected in such common features of synucleins as a native unfolded state in physiological solutions, reversible binding to lipid vesicles, and localization in presynaptic terminals (13, 25, 31). However, the C-terminal regions of synucleins, although all highly acidic, are rather different (7, 29, 52). It is perhaps this structural diversity that leads to differences in the behavior of synucleins in vitro and in various in vivo model systems. Consistent with the finding that β-synuclein and γ-synuclein are much less fibrillogenic than α-synuclein (4, 47, 55), aggregates of these two proteins are not constituents of Lewy bodies or other histopathological hallmarks of synucleinopathies, although abnormal β- and γ-synuclein-positive structures have been observed in several cases (15, 17, 49). Recent in vitro studies have also shown that both β- and γ-synuclein are able to inhibit fibrillation of α-synuclein (40, 55). In transgenic mice overexpression of β-synuclein reduces the severity of neurodegenerative alterations and the number of α-synuclein-positive interneuronal inclusions caused by α-synuclein overexpression (23). Changes of expression of all three synucleins in brain areas affected in neurodegenerative diseases have been reported (44). Previously we demonstrated that overexpression of α-synuclein, but not γ-synuclein, kills sensory neurons in primary cultures (6, 45). Moreover, it has been shown that γ-synuclein is able to block JNK signaling, a pathway whose activation is commonly associated with induction of apoptosis (39). These observations suggest that the correct balance of synucleins might be important for survival of at least some populations of neurons and that decreased expression of γ-synuclein might have a proapoptotic effect. The obvious way to investigate this is to assess whether the absence of γ-synuclein affects neurons that normally express these two proteins. In different vertebrate species, high levels of γ-synuclein mRNA are detected from the early stages of embryonic development in two neuronal populations, motoneurons and peripheral sensory neurons (7, 52), and α-synuclein is also expressed in these neurons (18, 32, 52; our unpublished observations). Moreover, in transgenic mice overexpression of

* Corresponding author. Mailing address: Department of Preclinical Veterinary Sciences, University of Edinburgh, Summerhall, Edinburgh EH9 1QH, United Kingdom. Phone: 44-131-6506105. Fax: 44-131-6506576. E-mail: v.buchman@ed.ac.uk.

† Present address: Department of Biological Chemistry, School of Medicine, University of Athens, 115 27 Athens, Greece.

‡ Present address: Department of Haematology, Cambridge Institute for Medical Research, University of Cambridge, Cambridge CB2 2XY, United Kingdom.

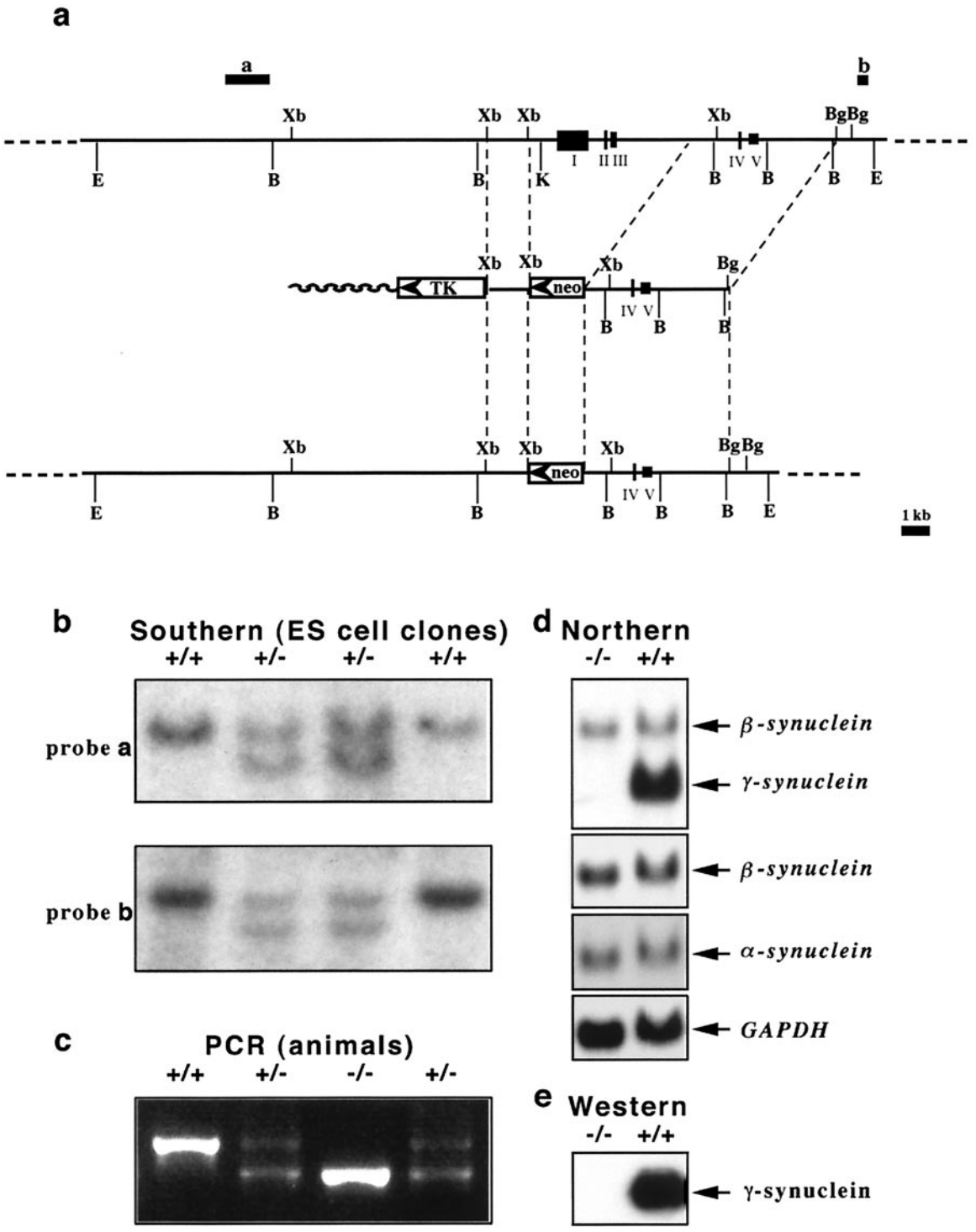

FIG. 1. Targeted inactivation of the mouse γ-*synuclein* gene. (a) Scheme for deletion of exons I, II, and III and promoter region of the mouse γ-*synuclein* gene by homologous recombination. The organizations of the wild-type genomic locus (top), targeting vector (middle), and resulting knockout locus (bottom) are shown. Restriction endonuclease sites: E, *Eco*RI; B, *Bam*HI; Xb, *Xba*I; K, *Kpn*I; Bg, *Bgl*II. Hybridization probes a and b, which were used for the analysis of homologous recombination, are also shown. (b) Examples of analysis of homologous recombination in ES cell lines by Southern hybridization. DNAs from four neomycin-resistant ES cell lines were digested with *Eco*RI and hybridized with either probe a or probe b. Only a 20-kb wild-type band is revealed in two clones with random insertion of a *PGK-neo* cassette, and the homologous recombination in two other clones results in the appearance of a 17-kb band. Similar results were obtained when DNA was digested with *Bam*HI and hybridized with probe c. (c) Example of PCR-based genotyping of mice from a litter of two heterozygous parents. (d) Expression of mRNAs encoding members of the synuclein family in the retinas of wild-type and γ-synuclein null mutant mice. Results of Northern hybridization with a full-length mouse γ-*synuclein* cDNA probe, a mouse β-*synuclein*-specific probe, a mouse α-*synuclein*-specific probe, and a *GAPDH* (glyceraldehyde-3-phosphate dehydrogenase) probe are shown. Note that under the hybridization and washing conditions used, the γ-*synuclein* cDNA probe cross-hybridized with β-*synuclein* transcript (upper panel). High-stringency washes completely eradicated this hybridization signal, with no effect on hybridization with γ-*synuclein* transcript. (e) A Western blot of 10 μg of total spinal cord proteins of wild-type and γ-synuclein null mutant mice was probed with mouse γ-synuclein-specific SK23 antibody.

α-synuclein leads to pathological changes in spinal and brain stem motoneurons (19, 30, 56), suggesting that these neurons are susceptible to changes in the metabolism of synucleins. Therefore, we studied populations of motoneurons and peripheral sensory neurons in γ-synuclein null mutant mice, which we produced.

MATERIALS AND METHODS

Generation of γ-*synuclein* null mutant mice. To generate a targeting vector, a 1.2-kb *Xba*I-*Xba*I fragment from lambda genomic clone PS92 (2) was cloned as a short arm into an *Xba*I site of the pPNT vector (54) between *PGK-TK* and *PGK-neo* cassettes. The resulting plasmid was digested with *Sse*8387I, blunted with the Klenow fragment of DNA polymerase I, further digested with *Xho*I, and used as a vector for ligation with a long arm. DNA of lambda genomic clone PS91 (2) was digested with *Bgl*II, blunted with Klenow fragment of DNA polymerase I, and further digested with *Sal*I, and a 4-kb fragment was used as a long arm in our targeting vector (Fig. 1a). For electroporation of 129Ola mouse ES cells (clone E14Tg2a; a gift of A. Smith, Centre for Genome Research, University of Edinburgh), DNA of the resulting targeting vector was linearized by digestion with *Not*I. After electroporation and selection, G418- and ganciclovir-resistant ES cell clones were checked for correct homologous recombination by Southern hybridization analysis of *Eco*RI-digested (for probes a and b in Fig. 1a) or *Bam*HI-digested (for probe c) DNA. Suitable clones were injected into blastocysts of C57Bl6J mice (Charles River). All procedures involved in generation of mutant mice were carried out according to the United Kingdom Animals (Scientific Procedures) Act (1986) and other Home Office regulations under specific-pathogen-free conditions. The presence of a mutant allele in animals was checked by PCR analysis of DNA extracted from mouse tail biopsies. A common upstream primer (5′-AGTCCTGGCACCTCTAAGCA-3′) and primers specific for the wild-type allele (5′-GGGCTGATGTGTGGCTATCT-3′) and the *PGK-neo* cassette in the mutant allele (5′-GAAGAACGAGATCAGCAGCC-3′) were used for amplification. Forty cycles of 45 s at 95°C, 30 s at 56°C, and 60 s at 72°C were carried out. The presence of 480-bp (for the wild-type allele) and 397-bp (for the mutant allele) amplification products in the reaction mixture was checked by electrophoresis in a 1.5% agarose gel. Heterozygous animals were used for at least six further generations of backcrosses with C57BL6J mice before null mutant, wild-type, and heterozygous littermates were produced for further studies by breeding heterozygous males and females. The mutant mouse strain was registered in the Mouse Genome Information database under the official name (B6-TgHSNCG^{tm1VLB}).

α-*synuclein* null mutant mice. Generation of α-*synuclein* mutant mice was described previously (1). We backcrossed these mice with C57Bl6J mice for at least six generations before setting up intercrosses to produce null mutant, wild-type, and heterozygous littermates.

Expression studies. Extraction of RNA from mouse tissues, Northern blotting, and preparation of labeled probes were carried out as described previously (7, 36).

Affinity-purified polyclonal rabbit SK23 antibody generated against a C-terminal peptide of mouse γ-synuclein (persyn) was used at a 1:500 dilution for Western blotting and enhanced chemiluminescence detection of this protein in total cell lysates as described earlier (7, 36). For immunohistochemistry, adult mouse brains and embryonic day 12 (E12), E15, and E18 embryos were fixed in 4% paraformaldehyde–phosphate-buffered saline (PBS) or Carnoy's fixative (60% ethanol, 30% chloroform, 10% glacial acetic acid) at 4°C overnight following dehydration in alcohol series and embedding in paraffin blocks. Eight-micrometer-thick sections were cut with a Leica or Microm microtome and mounted on SuperFrost slides (BDH, Poole, United Kingdom) for conventional staining or on Gold Seal slides (Gold Seal Products, Portsmouth, N.H.) for immunostaining. The paraffin sections were cleared in xylene and rehydrated through a graded alcohol series. Endogenous peroxidase activity was quenched by incubating the slides in 3% H_2O in methanol for 20 min. After being washed with PBS, the tissues were blocked in 10% horse or goat serum and 0.4% Triton X-100 in PBS for 1 h at room temperature. Incubation with a 1:40 dilution of SK26 anti-mouse γ-synuclein antibody was carried out at 4°C overnight. Detection of immune complexes with biotinylated anti-rabbit antibody and avidin-peroxidase complex from the Vectastain ABC kit (Vector Laboratories, Peterborough, United Kingdom) and diaminobenzidine (Fast 3,3′-diaminobenzidine tablet sets; Sigma, St. Louis, Mo.) as a substrate was carried out according to the manufacturer's instructions. Motor nuclei were identified by staining of alternate sections with hematoxylin-eosin (Raymond A Lamb, London, United Kingdom) and a goat antibody against choline acetyltransferase (Chemicon, Temecula, Calif.) at a 1:100 dilution. In the latter case, anti-goat secondary antibody was used for detection.

Whole-mount immunofluorescence. Mouse triangularis sterni muscle was dissected in PBS and fixed in 4% paraformaldehyde–PBS for 20 min, followed by incubation with AlexaFluor 647-conjugated μ-bungarotoxin (5 μg/ml in PBS) for 30 min. After washing in PBS and blocking and permeabilization for 1 h in 1% bovine serum albumin–0.4% lysine–0.5% Triton X-100 in PBS, samples were incubated overnight with primary antibodies diluted in the same buffer at 4°C. Mouse monoclonal anti-neurofilament M (clone 2H3; Developmental Studies Hybridoma Bank, Iowa City, Iowa) and anti-synaptic vesicles (clone SV2; Developmental Studies Hybridoma Bank) antibodies were used at a 1:200 dilution, and rabbit polyclonal SK23 antibody was used at a 1:40 dilution. After several washes, incubation with 1:200-diluted secondary antibodies (fluorescein isothiocyanate-conjugated goat anti-rabbit immunoglobulins and tetramethyl rhodamine isocyanate-conjugated goat anti-mouse immunoglobulins, both from Jackson ImmunoResearch Laboratories, West Grove, Pa.) was carried out for 3 h at room temperature, followed by extensive washing and mounting in Vectashield (Vector Laboratories, Burlingame, Calif.). Images were obtained with a Zeiss LSM 510/Axioplan 2 confocal microscope.

DRG neuron counts. The spinal columns from P2 mice were fixed and embedded as described above. Serial 8-μm-thick longitudinal sections were cut, mounted on SuperFrost slides (BDH), cleared in xylene, rehydrated through a graded alcohol series, and stained with 0.1% cresyl violet acetate (Sigma). Lumbar L6 dorsal root ganglia (DRG) were identified by using characteristic tissue landmarks on sections. Neurons were identified by virtue of the Nissl substance and their large, round, pale-stained nuclei (27). Neurons in the L6 DRG displaying a prominent nucleolus were counted on every eighth section. The neuronal number was quantified by using a digital stereology system that employs a combination of the optical dissector and volume fraction-Cavalieri methods (Kinetics Imaging, Bromborough, United Kingdom). All counts were carried out blindly by a person unaware of animal genotypes.

Motoneuron counts. Adult mouse brains were fixed and processed as described above for expression studies. The whole brain stem was sectioned into 8-μm-thick sections, which were mounted on SuperFrost slides. Rehydrated sections were stained in a 1% solution of neutral red (Raymond A Lamb) in distilled water for 30 min, followed by dehydration and mounting as described above. A stereological fractionator method (22), which allows estimation of the number of particles independent of the volume of the structure that the particles are part of and is not affected by tissue shrinkage during processing, was used to assess the number of motoneurons in five motor nuclei of the brain stem. Large (~20 μm in diameter) neurons displaying a prominent nucleolus were counted in total on every fifth section throughout the nucleus; the first section for counting was randomly chosen from the first five sections that included this nucleus.

Nerve fibers counts. Anesthetized animals were transcardially perfused with heparinized saline and then 2.5% glutaraldehyde–2% paraformaldehyde–0.1 M sodium cacodylate buffer (pH 7.3)–1 mM $CaCl_2$ for 5 min. The saphenous nerve was removed and fixed for 2 h in the same fixative, postfixed in OsO_4, and embedded in araldite. One-micrometer resin sections were prepared and stained with toluidine blue for light microscopy to measure the area of the nerve cross-section. Ultrathin 80-nm transverse sections were stained with uranyl acetate and lead citrate, mounted onto copper slot grids, and examined on a transmission electron microscope (Phillips BioTwin; FEI, Cambridge, United Kingdom). Myelinated A-fibers and unmyelinated C-fibers were identified and counted as described previously (57). The densities of both types of fibers were calculated after counting of 12 to 15 randomly chosen electron microscope images and multiplied by the area of the nerve cross-section.

Primary neuronal cultures. Cultures from trigeminal and superior cervical ganglia were prepared as described previously (42) and maintained in neurobasal medium with B27 complement (Invitrogen, Carlsbad, Calif.). The number of neurons attached to each culture dish within a 12- by 12-mm square was counted 3 h after plating and was taken as the initial number of neurons (100%). In experiments with proteasome inhibitors and metal ions, the initial count was carried out 24 h after plating. In all cases drugs were added to cultures immediately after the initial count. The number of surviving neurons in the same area was counted 24 and 48 h later and was expressed as a percentage of the initial count.

Behavioral tests. All experiments were carried out in accordance with the United Kingdom Animals (Scientific Procedures) Act (1986). Behavioral testing was carried out prior to surgery to establish a baseline for comparison to post-surgical values, as described in detail previously (5, 11). The procedure of chronic constriction injury (CCI) to the sciatic nerve was modified for mice from a procedure described previously for rats (3). In brief, adult male mice (90 to 120 g) were anaesthetized with sodium pentobarbital (Sagatal; Rhône Merieux,

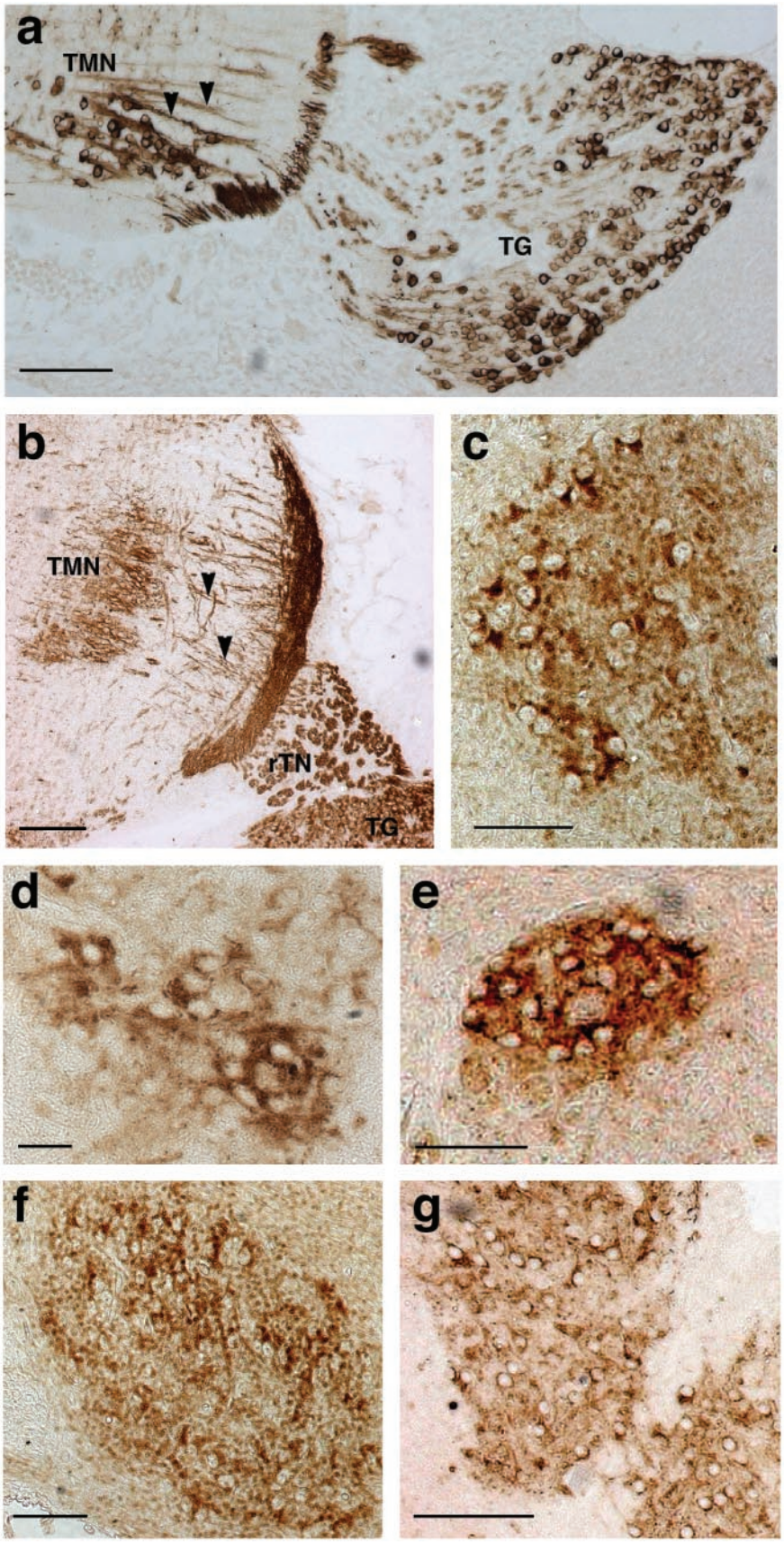
a
TMN
TG
b
TMN
rTN
TG
c
d
e
f
g

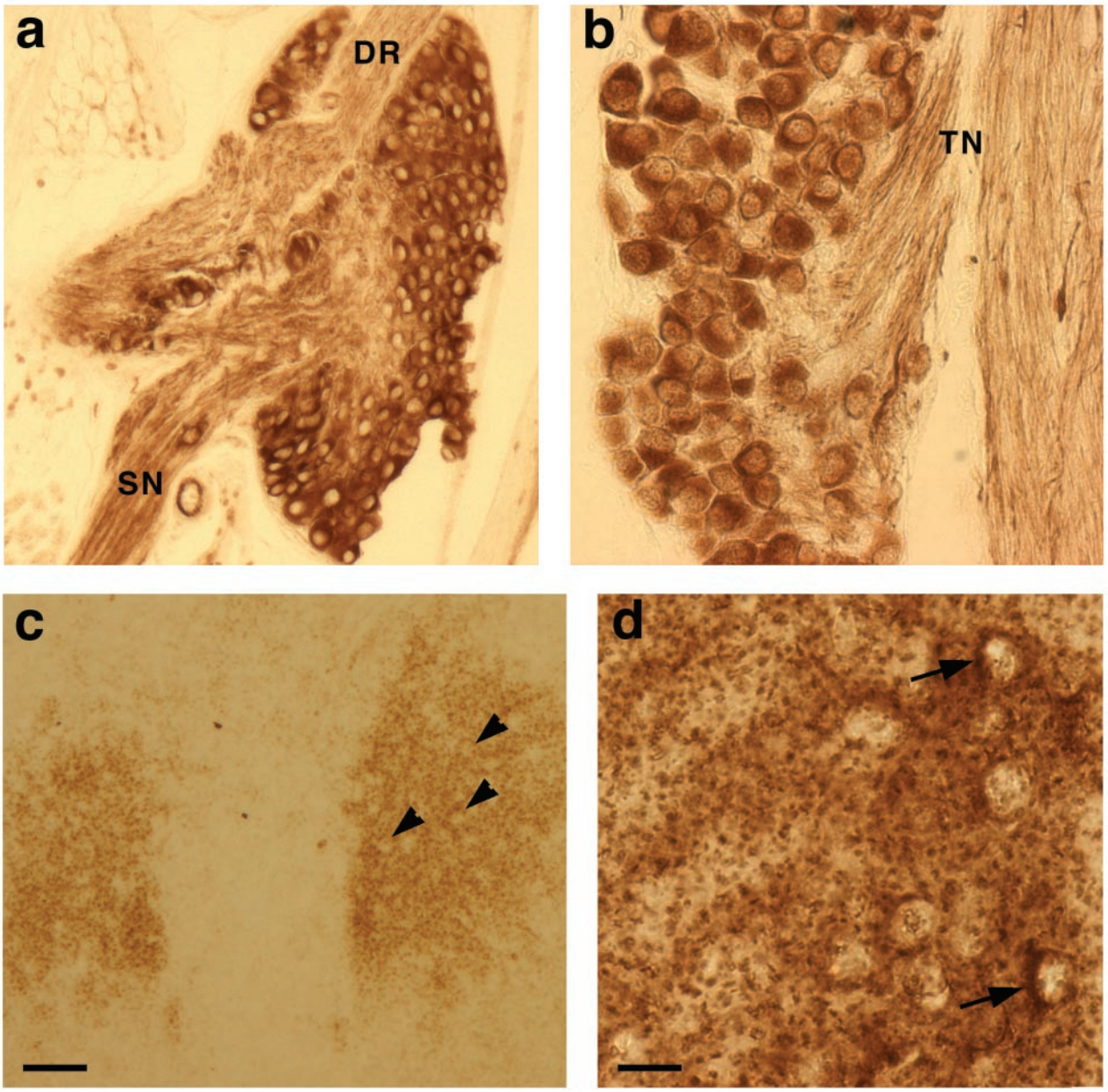

FIG. 3. γ-Synuclein in postnatal mouse sensory and motoneurons. γ-Synuclein is localized in the cytoplasm of cell bodies of mouse P2 DRG (a) and trigeminal ganglion (b) neurons as well as in nerve fibres in the dorsal root (DR), spinal nerve (SN), and trigeminal nerve (TN). In P2 oculomotor nucleus (c), only γ-synuclein-negative cell bodies (arrowheads) are seen on the background of neuropil staining, whereas in P2 trigeminal motor nucleus (d), cytoplasmic staining can be detected in some neurons (arrows). Bars, 100 μm (a and c) and 20 μm (b and d).

Essex, United Kingdom) (0.06 ml/100 g, intraperitoneally) supplemented with halothane-O_2 (Zeneca, Cheshire, United Kingdom). Under aseptic conditions, the right sciatic nerve was exposed proximal to the trifurcation, at mid-thigh level, and three chromic cat gut ligatures were tied to loosely constrict the nerve. The overlying muscle and skin were closed with sutures, and the animals were allowed to recover before reflex testing recommenced. Thermal hyperalgesia was monitored by using noxious radiant heat (30 to 55°C) (Hargreaves' thermal device; Linton Instruments, Diss, United Kingdom) applied to the mid-plantar glabrous surface of the hind paw. The withdrawal response latency was characterized as a brief paw flick, and a standard cutoff latency of 20 s prevented tissue damage. Mechanical allodynia was measured as the threshold for paw withdrawal in response to graded mechanical stimuli applied to the mid-plantar glabrous

FIG. 2. γ-Synuclein in embryonic mouse sensory and motoneurons. Anti-γ-synuclein staining of E12 (a) and E15 (b) trigeminal motor nuclei and trigeminal ganglia and of E18 trigeminal motor nucleus (c), E18 oculomotor nucleus (d), E18 trochlear nucleus (e), E18 facial nucleus (f), and E18 hypoglossal nucleus (g) is shown. All nuclei contain labeled neuronal cell bodies, but dotted neuropil stain becoming also obvious in all ganglia at E18. Arrowheads show γ-synuclein-positive axons of E12 and E15 motoneurons of the trigeminal motor nucleus (TMN). Sensory neurons of the trigeminal ganglion (TG) are also intensively stained, as is the root of the trigeminal nerve (rTN). Bars, 100 μm (a, c, e, and f), 200 μm (b and g), and 50 μm (d).

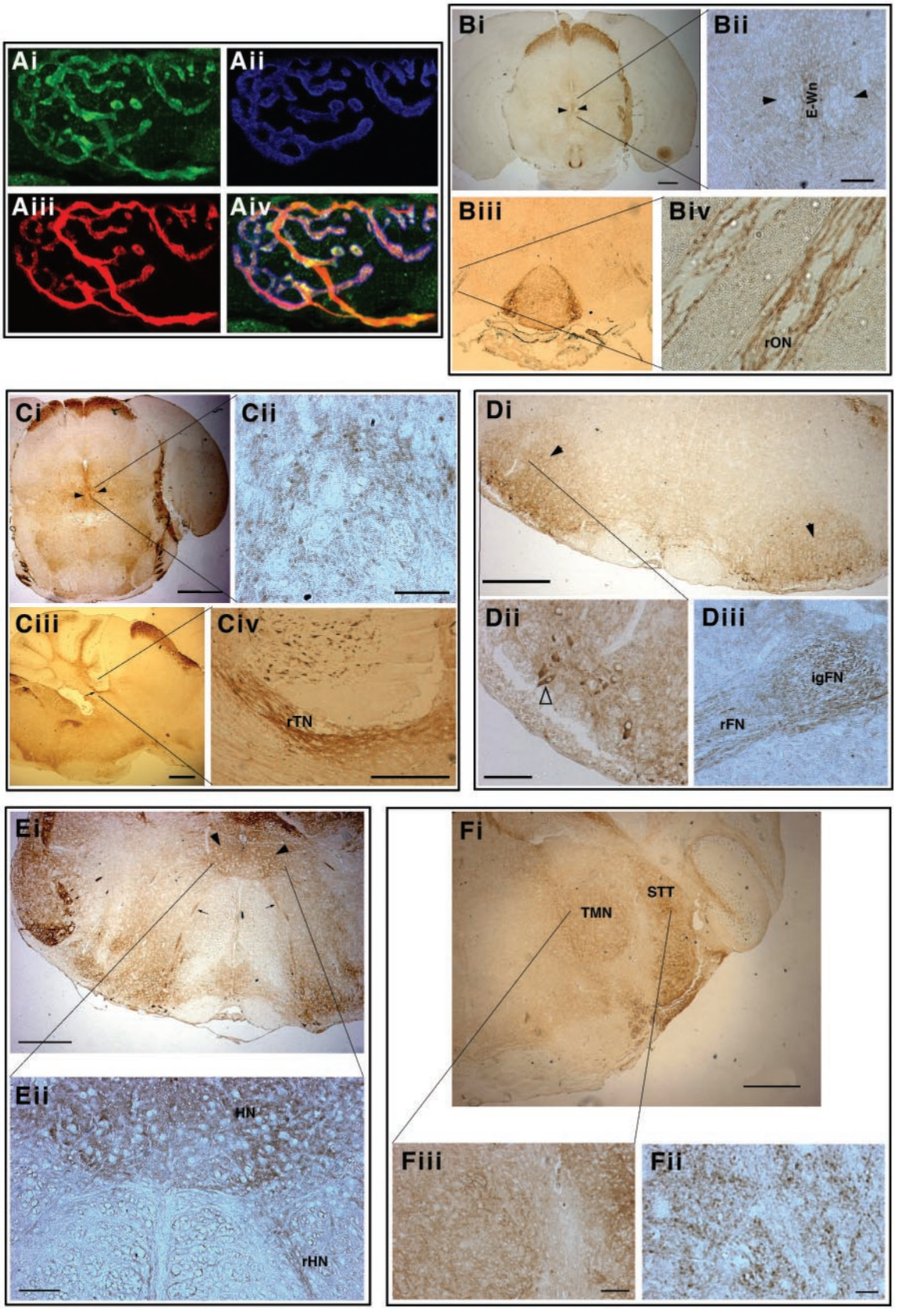
Ai
Aii
Aiii
Aiv
Bi
Bii
E-Wn
Biii
Biv
rON
Ci
Cii
Ciii
Civ
rTN
Di
Dii
Diii
igFN
rFN
Ei
Eii
HN
rHN
Fi
STT
TMN
Fiii
Fii

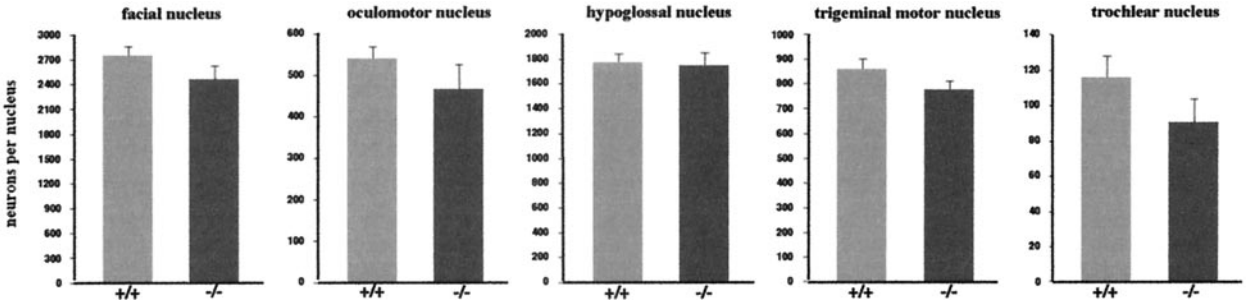

FIG. 5. Average total numbers of motoneurons in brain stem motor nuclei of wild-type (+/+) and γ-*synuclein* null mutant (-/-) adult mice. Means and standard errors from data obtained from analysis of at least 10 nuclei for each genotype are shown. Statistical analysis (two-tailed, unpaired Student's *t* test) showed no significant difference in cell numbers between the two genotypes for all nuclei ($P > 0.5$).

surface of the hind paw with calibrated von Frey filaments (Stoelting, Wood Dale, Ill.). The threshold was defined as the pressure (force per unit area) that caused foot withdrawal five times in every 10 applications, repeated at 1- to 2-s intervals. The pressure applied to the hind limb by the von Frey filaments is calibrated as force (millinewtons) divided by the area over which it is applied (square millimeters).

RESULTS

Generation of γ-*synuclein* null mutant mice. Mouse strains with a targeted deletion of the first three exons of the mouse γ-*synuclein* gene (Fig. 1) were generated from three independent ES cell clones as described in Materials and Methods. Two of these strains were used in this study, and because the results were identical, the experimental data obtained with both strains were combined. Mice lacking the γ-*synuclein* gene were viable and fertile and did not show any obvious abnormalities in development, behavior, or gross morphology of the nervous system (data not shown). Western blotting (Fig. 1e) and immunohistochemistry (not shown) with an antibody specific to the C-terminal peptide of mouse γ-synuclein showed a complete absence of the protein in all tissues of null mutant mice. Northern hybridization of RNAs from various tissues confirmed complete inactivation of γ-*synuclein* gene function in null mutant mice, which was not accompanied by compensatory increases of α- or β-*synuclein* mRNA levels (Fig. 1d and data not shown).

In the absence of an obvious phenotypic manifestation of the null mutant genotype in γ-synuclein knockout mice, we carried out comparative studies of several neuronal populations with wild-type and null mutant mice. Motoneurons and peripheral sensory neurons were chosen because both populations normally express high levels of γ-*synuclein* mRNA (7) but, as shown below, display different intracellular compartmentalization of γ-synuclein.

Developmental changes of γ-synuclein compartmentalization in motoneurons. Previously we have demonstrated by in situ hybridization high levels of γ-*synuclein* mRNA expression in spinal and cranial motoneurons from early stages of mouse and rat embryonic development (7). However, neither the abundance nor the intracellular localization of γ-synuclein protein in these neurons has been studied. Using a specific antibody which recognizes the C-terminal peptide of mouse γ-synuclein, we now demonstrated that the protein expression pattern follows the mRNA expression pattern but that dramatic changes in compartmentalization of γ-synuclein within motoneurons take place during postnatal development. Immunohistochemistry was performed on sagittal as well as coronal paraffin sections of mouse embryos of different developmental stages and adult mouse brains. To identify oculomotor, trochlear, facial, hypoglossal, and trigeminal motor nuclei, adjacent sections were stained with hematoxylin-eosin and an antibody against choline acetyltransferase, a motoneuron marker (see Materials and Methods). From the early stages (E12) and throughout the embryonic development, γ-synuclein is localized in both motoneuron cell bodies and axons (Fig. 2 and data not shown). However, at E18, in addition to cytoplasmic staining, a dotted neuropil staining became evident in all studied motor nuclei (Fig. 2c to g). The pattern is completely different in motor nuclei of postnatal, particularly adult, mouse brain.

FIG. 4. γ-Synuclein in adult mouse motoneurons. (A) γ-Synuclein in motor axons and nerve terminals at the neuromuscular synapse. Triple immunofluorescent staining of whole-mount preparations of mouse traingularis sterni muscle is shown. γ-Synuclein (Ai, green) is colocalized with neurofilaments in the axon and SV2 in presynaptic terminals (Aiii, red) but not with acetylcholine receptors on postsynaptic membrane (Aii, blue [stained with AlexaFluor 647-conjugated μ-bungarotoxin]). Three images are merged in panel Aiv. (B) γ-Synuclein in oculomotor nuclei (arrowheads) and the root of oculomotor nerve (rON). A higher magnification shows axonal staining in the nerve root (panel Biv), the absence of γ-synuclein in cell bodies of motoneurons, and positive staining of neuronal cell bodies in the median Edinger-Westphal nucleus (E-Wn, panel Bii). (C) γ-Synuclein in trochlear nuclei (arrowheads in panel Ci) and the root of trochlear nerve (arrow in panel Ciii and rTN in panel Civ). A higher magnification shows intense staining of motoneuron axons in the nerve (Civ) and only a dotted neuropil staining in the nucleus (Cii). (D) γ-Synuclein in facial nuclei (arrowheads) and the facial nerve. Axonal staining is evident in the internal genu (IgFN) and the root (rFN) of the nerve (panel Diii). A higher magnification reveals γ-synuclein in the cytoplasm of a few motoneurons (open arrowhead in panel Dii). (E) γ-Synuclein in hypoglossal nuclei (arrowheads in panel Ei and HN in panel Eii) and the root of hypoglossal nerve (rHN in panel Eii). A higher magnification shows positive staining of the nerve root and neuropil staining in the nucleus (Eii). (F) γ-Synuclein in the trigeminal motor nucleus (TMN) and the spinal trigeminal tract (STT). Neuronal cell bodies are not stained; only dotted neuropil staining is evident at the highest magnification (Fiii).

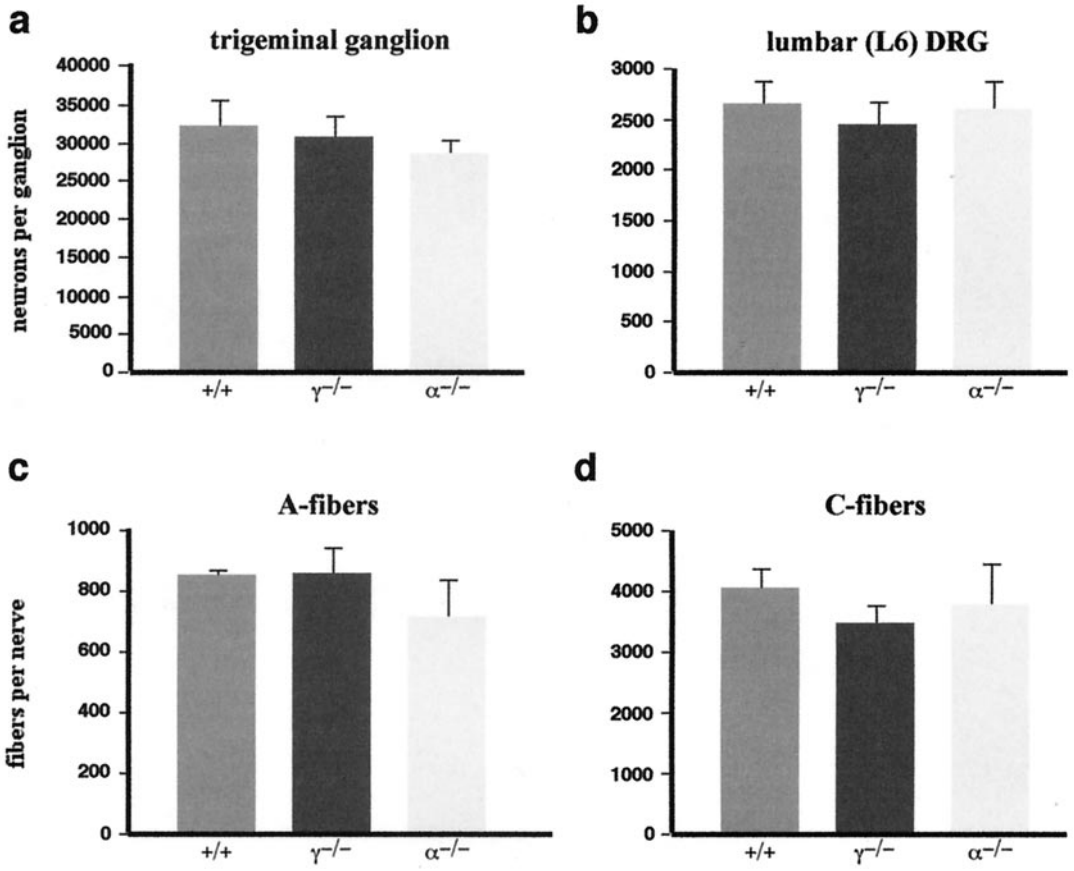

FIG. 6. Numbers of sensory neurons and nerve fibers in wild-type and null mutant mice. (a and b) Average total number of neurons in trigeminal ganglia (a) and L6 lumbar DRG (b) of wild-type (+/+), γ-*synuclein* null mutant ($\gamma^{-/-}$), and α-*synuclein* null mutant ($\alpha^{-/-}$) P2 mice. Means and standard errors of data obtained from analysis of at least 10 ganglia for each genotype are shown. Statistical analysis (Kruskal-Wallis one-way analysis of variance) showed no significant difference in cell numbers between all three genotypes for both ganglia ($P > 0.6$). (c and d) Average total numbers of myelinated A-fibers (c) and unmyelinated C-fibers (d) in adult mouse saphenous nerves. Means and standard errors of data obtained from analysis of at least five nerves for each genotype are shown. Statistical analysis (Kruskal-Wallis one-way analysis of variance) showed no significant difference in numbers for both types of fibers between all three genotypes ($P > 0.4$).

At postnatal day 2 (P2), only neuropil staining (Fig. 3c) or very few neurons with γ-synuclein-positive cytoplasm on the background of neuropil staining (Fig. 3d) are evident in these nuclei. In adult brain all motor nuclei (with the exception of the facial nucleus, where a few neurons still display positive cytoplasmic staining) show a complete absence of γ-synuclein in the cytoplasm of neuronal cell bodies, but axons in all studied motor nerve roots display intense γ-synuclein immunoreactivity (Fig. 4). Using immunofluorescence, we clearly demonstrated that γ-synuclein is present not only in axons but also in presynaptic terminals of motoneurons in neuromuscular junctions (Fig. 4A).

Intracellular localization of γ-synuclein in mouse sensory neurons. As in motoneurons, in sensory neurons of embryonic peripheral ganglia γ-synuclein is distributed throughout the cytoplasm of cell bodies and axons (Fig. 2 and data not shown). However, in contrast to the case for motoneurons, γ-synuclein compartmentalization in sensory neurons does not change during late embryonic and postnatal development. Postnatal neurons of DRG and cranial sensory ganglia display intensive immunostaining of their cell bodies as well as nerve fibers with anti-γ-synuclein antibody (Fig. 3a and b and data not shown).

Numbers of motoneurons in cranial nuclei of wild-type and γ-*synuclein* null mutant mice. Serial coronal sections of adult mouse brain were prepared and stained, and motoneurons were counted in five cranial nuclei as described in Materials and Methods. In neither of these ganglia were statistically significant differences in the number of neurons between wild-type and γ-*synuclein* null mutant mice found (Fig. 5).

Numbers of sensory neurons in DRG and trigeminal ganglia of wild-type and null mutant mice. The number of neurons in L6 lumbar DRG and trigeminal ganglia was assessed in P2 mice, after the period of physiological cell death in these ganglia. Serial longitudinal sections of the lumbar part of the spinal column and transverse sections of the head were stained and neurons were counted as described in Materials and Methods. Figure 6a and b show that the absence of γ-synuclein does not have an effect on the number of neurons in both sensory ganglia. Similarly, no effect of the absence of α-synuclein on the neuronal complement in these ganglia was found. Mice with a targeted inactivation of the α-*synuclein* gene have been described previously (1), but for this work they were further backcrossed with C57BL6J mice (as described in Materials and

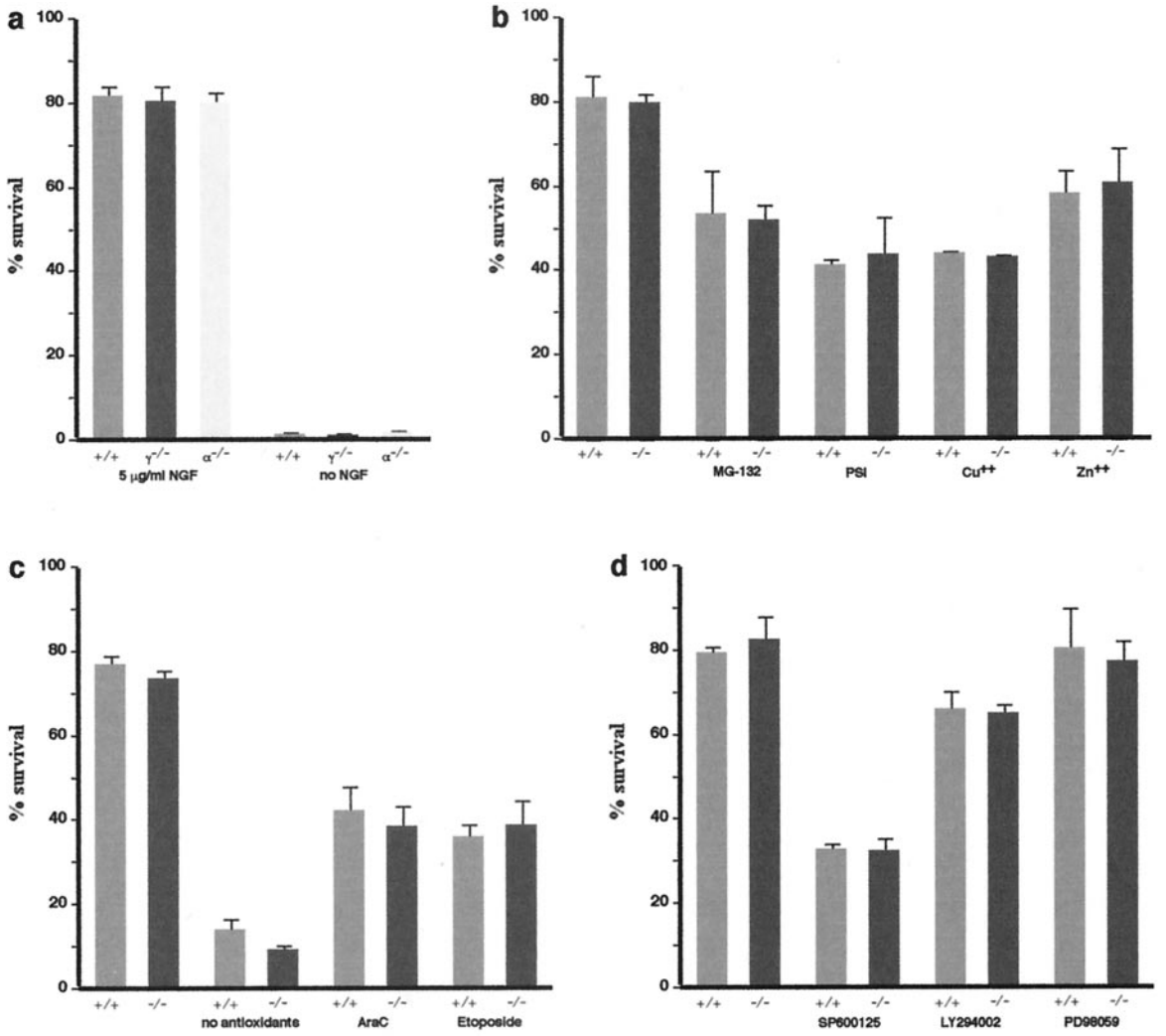

FIG. 7. Survival of P2 mouse trigeminal ganglion neurons in dissociated primary culture. Cultures were prepared and treated with drugs as described in Materials and Methods. Bar charts illustrate survival of neurons 48 h after initial count and addition of drugs. The number of surviving neurons is expressed as a percentage of the initial count. Means and standard errors of data obtained from analysis of at least six culture dishes for each genotype in two independent experiments are shown. (a) Both γ-synuclein-deficient ($\gamma^{-/-}$) and α-synuclein-deficient ($\alpha^{-/-}$) neurons have the same survival rate as wild-type (+/+) neurons in the presence of nerve growth factor (NGF) and are unable to survive in its absence ($P > 0.8$, Kruskal-Wallis one-way ANOVA). (b to d) Various treatments have the same effect on γ-synuclein deficient (−/−) neurons as they have on wild-type (+/+) neurons ($P > 0.5$ for all conditions; two-tailed, unpaired Student's t test). Proteasome inhibitors (5 μM MG-132 or 10 μM proteasome inhibitor I [PSI]) or heavy metal ions (30 μM $CuSO_4$ or 75 μM $ZnSO_4$) were added to neurons after the initial count at 24 h after plating (b). In one set of experiments neurons were plated in neurobasal medium supplemented with B27 without antioxidants (c). In other cases, DNA-damaging agents (10 μM cytosine arabinoside [AraC] or 10 μM Etoposide) or inhibitors of the JNK signaling pathway (20 μM SP600125), ERK signaling pathway (20 μM PD98059), or phosphatidylinositol 3-kinase signaling pathway (20 μM LY294002) were added to neurons after the initial count at 3 h after plating (c and d).

Methods) to obtain a colony with a genetic background similar to that of the γ-*synuclein* null mutant mice.

Numbers of nerve fibers in saphenous nerves of wild-type and null mutant mice. To determine whether the absence of synucleins affected growth and myelinization of axons of sensory neurons, we examined the mouse saphenous nerve, which contains mostly afferent sensory nerve fibers, and counted the numbers of myelinated A-fibers and unmyelinated C-fibers. No differences in the general ultrastructural morphology of the fibers (not shown) or in their numbers (Fig. 6c and d) in γ-*synuclein* and α-*synuclein* null mutant mice compared to the wild-type mice were found.

Survival in culture of peripheral nervous system neurons of wild-type and null mutant mice. Although no differences in neuron numbers in DRG or trigeminal ganglia of wild-type, γ-*synuclein*, and α-*synuclein* null mutant mice were found, it was feasible to check whether neurons with an incorrect balance of synucleins are more sensitive to various stresses than wild-type neurons. For this we compared the survival of neurons from peripheral ganglia of null mutant and wild-type mice in dissociated primary cultures. Dissociated cultures of P2 trigeminal ganglion neurons were prepared and neuronal survival was assessed as described previously (42). Survival characteristics of γ-synuclein- and α-synuclein-deficient neurons were

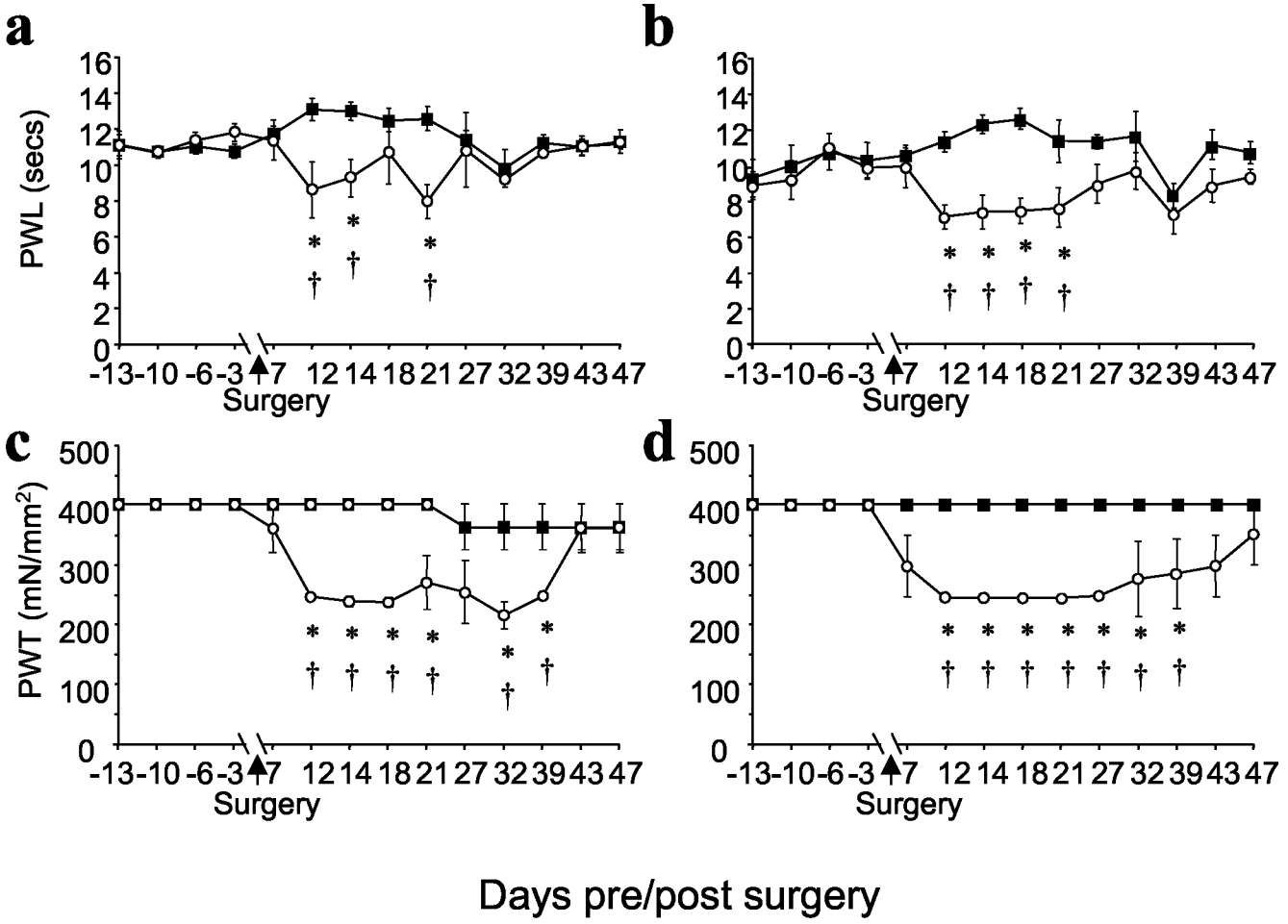

FIG. 8. Behavioral analysis of mice with CCI to the sciatic nerve. Data show mean (± standard error of the mean) responses taken over a period of up to 13 days before and every 2 to 6 days following surgery in wild-type mice (a and c) ($n = 9$) and γ-*synuclein* null mutant mice (b and d) ($n = 6$). (a and b) Paw withdrawal latency (PWL) from a noxious thermal stimulus (Hargreaves' thermal stimulator) ipsilateral to CCI (○) showed significant differences between postoperative and preoperative values (†, $P < 0.05$; Kruskal-Wallis one-way analysis of variance) and from postoperative, contralateral (■) values (*, $P < 0.05$ by Student's t test) for both wild-type (a) and mutant (b) mice. No thermal hyperalgesia was seen on the contralateral side. (c and d) Paw withdrawal thresholds (PWT) from mechanical stimulation (von Frey filaments) showed significant differences between postoperative and preoperative values on the side ipsilateral (○) to CCI (†, $P < 0.05$; Dunn's method analysis of variance on ranks) and between postoperative ipsilateral and contralateral (■) values (*, $P < 0.05$, Mann-Whitney U-test) for both wild-type (c) and mutant (d) mice.

indistinguishable from those of wild-type neurons; they survived similarly well in the presence of nerve growth factor and failed to survive in its absence (Fig. 7a). Similar results were obtained for P2 superior cervical ganglion neurons (data not shown). It has been shown previously that certain types of cells with modified expression of synucleins, particularly dopaminergic neurons overexpressing α-synuclein, have normal survival characteristics under optimal culture conditions but are substantially more susceptible to stresses (37, 38, 41, 50, 51). To determine whether the absence of γ-synuclein renders neurons more sensitive to various toxic insults, we cultivated P2 trigeminal neurons in the absence of antioxidants or in the presence of DNA-damaging agents (Fig. 7c), proteasome inhibitors, heavy metal ions (Fig. 7b), and inhibitors of major intracellular signaling pathways (Fig. 7d) in the medium. None of these treatments revealed differences in the survival of γ-synuclein-deficient neurons compared to wild-type neurons.

Sensory reflexes and effects of CCI in wild-type and γ-*synuclein* null mutant mice. The behavioral reflex responses of adult male γ-*synuclein* null mutant and wild-type littermate mice to noxious radiant heat and graded mechanical stimuli were studied as described in Materials and Methods. In both tests the behaviors of mice from these two groups were indistinguishable (Fig. 8). To examine the effects of sciatic nerve injury on behavioral reflex responses, we used the CCI model of neuropathic pain. Over 7 to 10 days following CCI, wild-type and mutant mice progressively developed marked ipsilateral thermal hyperalgesia (reduced paw withdrawal latency) (Fig. 8a and b) and mechanical allodynia (reduced paw withdrawal threshold) (Fig. 8c and d). All responses from the contralateral hind limb remained unaltered. The time courses of recovery from the consequences of CCI were very similar for mice of both genotypes (Fig. 8). These results suggest that degeneration and regeneration of the injured nerve and neuronal plas-

ticity in the spinal cord are not compromised in γ-*synuclein* null mutant mice.

DISCUSSION

We have shown that in embryonic motoneurons γ-synuclein is uniformly distributed through the cytoplasm of cell bodies and axons. However, with the exception of a few neurons in the facial nucleus, the cytoplasm of cell bodies of motoneurons of the adult cranial somato- and branchiomotor nuclei is γ-synuclein negative, whereas their axons and synaptic boutons in neuromuscular junctions are intensively stained with anti-γ-synuclein antibody. Previously published in situ hybridization data demonstrated high levels of γ-*synuclein* mRNA in cranial motor nuclei of adult brain (7). Therefore, in motoneurons during postnatal development, γ-synuclein undergoes a compartmentalization shift, which might reflect a functional shift. Our results contradict recently published data (32) which demonstrated the presence of γ-synuclein in cell bodies of motoneurons in brain stem motor nuclei of adult rats. This might reflect a difference between species; however, a more plausible explanation is the difference in the antibodies used in the two studies. In the present study, a highly specific antibody generated against mouse γ-synuclein C-terminal peptide was used, whereas Li et al. (32) used an antibody generated against human recombinant γ-synuclein whose specificity has been checked with recombinant human synucleins but not with samples from null mutant animals.

It is not clear why some neurons of the adult facial nucleus do not follow the common rule and continue to accumulate γ-synuclein in the cytoplasm of their cell bodies. In this aspect they resemble peripheral sensory neurons, in which no developmental changes of intracellular compartmentalization of γ-synuclein take place and which have equally high levels of γ-synuclein in their cell bodies and processes during embryogenesis and postnatally. We found that both neural crest-derived DRG and placode-derived trigeminal sensory neurons have this unchanging pattern of γ-synuclein intracellular compartmentalization. Taken together, our expression studies demonstrated that between neurons expressing the highest levels of γ-synuclein throughout development, two subpopulations could be specified. The first includes peripheral sensory neurons and some motoneurons of the facial nucleus, which localize γ-synuclein in their cell bodies and axons at all developmental stages. Most other motoneurons of the brain stem nuclei comprise the second group, which is characterized by the developmental shift of γ-synuclein compartmentalization.

The high levels of expression suggest that γ-synuclein should have an important role in the development and function of sensory and motoneurons. Consequently, the loss of this protein could affect the morphology and/or physiology of animal sensory and motor systems. To check this, we produced mutant mice with complete inactivation of the γ-*synuclein* gene. Similarly to previously reported α-*synuclein* null mutants (1, 8, 46, 48), these mice showed no obvious phenotypical changes. Detailed studies of sensory and motoneurons in vivo and in vitro failed to detect any difference between γ-*synuclein* null mutant and wild-type mice. The number of neurons is not changed in either of the subpopulations described above, suggesting that proliferation, migration, differentiation, or programmed cell death is not affected by the absence of γ-synuclein. Consistently, survival of γ-synuclein-deficient neurons in primary culture is not different from survival of wild-type neurons. Moreover, the absence of γ-synuclein does not render these neurons either more or less sensitive to any of the survival-affecting factors studied so far. Because mid-brain dopaminergic neurons seem to be most vulnerable to changes of synuclein metabolism (references 10, 28, and 33 and references therein), it is feasible that this neuronal population might be more sensitive to changes in the synuclein ratio than motoneurons and sensory neurons. We are currently testing whether the absence of γ-synuclein affects survival of dopaminergic neurons in the substantia nigra and ventral tegmental area of null mutant mice.

It has been suggested previously that γ-synuclein could be involved in axonal growth and stabilization of axon architecture (6). However, we did not find differences in the morphology and number of myelinated or unmyelinated fibers in the saphenous nerves of mutant and wild-type mice. Sensory reflex thresholds were also intact in γ-*synuclein* null mutant mice. Nerve injury led to similar changes in sensory function in wild-type and mutant mice. Normalization of sensory function after nerve injury is believed to be associated with neuronal plasticity in the spinal cord and axonal regeneration processes in the injured peripheral nerve (9, 14, 21, 58). These processes require remodeling of the axonal cytoskeleton, including the neurofilament network, and involvement of γ-synuclein in regulation of neurofilament network integrity has been suggested previously (6). However, the time course of sensory recovery after CCI in γ-*synuclein* null mutant mice is the same as that in wild-type mice, which suggested that nerve regeneration and plasticity of early somatosensory pathways in γ-*synuclein* mutant mice were unaffected.

The most straightforward explanation of our results is that despite high levels of expression, γ-synuclein is not essential for the development and function of motor and peripheral sensory neurons. Nevertheless an alternative explanation is also possible. This function(s) could be vital for vertebrate organisms, and therefore effective mechanisms of protection against its loss have been developed in evolution. The presence of three closely related synucleins in all vertebrates and substantial overlapping of their expression patterns readily suggest that they are able to compensate for each other's function(s). It is unlikely that compensation for the loss of one synuclein function in mice is achieved by a simple increase of expression of other synucleins. We found no difference in the levels of mRNAs encoding the two remaining synucleins in several neuronal populations of γ-*synuclein* null mutant mice, and the same has been demonstrated before for α-*synuclein* null mutant mice (1). However, it is possible that it is not necessary to boost an already high level of synuclein expression, because changes in compartmentalization, posttranslational modifications, or interaction with other macromolecules could be required and sufficient for functional compensation. Detailed studies of these processes in synuclein null mutant mice as well as studies of double and triple synuclein mutants should shed more light on this problem and finally reveal the normal functions of these proteins.

ACKNOWLEDGMENTS

We are grateful to A. Smith and J. Ure for ES cells, help with the initial stages of generation of mutant mice, and valuable advice and to A. Oliver, S. Mitchell, and J. Wanless for excellent technical assistance.

This work was supported by grants from The Wellcome Trust.

REFERENCES

1. **Abeliovich, A., Y. Schmitz, I. Farinas, D. Choi-Lundberg, W. H. Ho, P. E. Castillo, N. Shinsky, J. M. Verdugo, M. Armanini, A. Ryan, M. Hynes, H. Phillips, D. Sulzer, and A. Rosenthal.** 2000. Mice lacking alpha-synuclein display functional deficits in the nigrostriatal dopamine system. Neuron **25:**239–252.
2. **Alimova-Kost, M. V., N. N. Ninkina, S. Imreh, N. V. Gnuchev, J. Adu, A. M. Davies, and V. L. Buchman.** 1999. Genomic structure and chromosomal localization of the mouse persyn gene. Genomics **56:**224–227.
3. **Bennett, G. L., and Y.-K. Xie.** 1988. A peripheral mononeuropathy in rat that produces disorders of pain sensation like those seen in man. Pain **33:**87–109.
4. **Biere, A. L., S. J. Wood, J. Wypych, S. Steavenson, Y. Jiang, D. Anafi, F. W. Jacobsen, M. A. Jarosinski, G. M. Wu, J. C. Louis, F. Martin, L. O. Narhi, and M. Citron.** 2000. Parkinson's disease-associated alpha-synuclein is more fibrillogenic than beta- and gamma-synuclein and cannot cross-seed its homologs. J. Biol. Chem. **275:**34574–34579.
5. **Blackburn-Munro, G., and S. M. Fleetwood-Walker.** 1999. The sodium channel auxiliary subunits beta1 and beta2 are differentially expressed in the spinal cord of neuropathic rats. Neuroscience **90:**153–164.
6. **Buchman, V. L., J. Adu, L. G. P. Pinõn, N. N. Ninkina, and A. M. Davies.** 1998. Persyn, a member of the synuclein family, influences neurofilament network integrity. Nat. Neurosci. **1:**101–103.
7. **Buchman, V. L., H. J. A. Hunter, L. G. P. Pinõn, J. Thompson, E. M. Privalova, N. N. Ninkina, and A. M. Davies.** 1998. Persyn, a member of the synuclein family, has a distinct pattern of expression in the developing nervous system. J. Neurosci. **18:**9335–9341.
8. **Cabin, D. E., K. Shimazu, D. Murphy, N. B. Cole, W. Gottschalk, K. L. McIlwain, B. Orrison, A. Chen, C. E. Ellis, R. Paylor, B. Lu, and R. L. Nussbaum.** 2002. Synaptic vesicle depletion correlates with attenuated synaptic responses to prolonged repetitive stimulation in mice lacking α-synuclein. J. Neurosci. **22:**8797–8807.
9. **Coggeshall, R. E., P. M. Dougherty, C. M. Pover, and S. M. Carlton.** 1993. Is large myelinated fiber loss associated with hyperalgesia in a model of experimental peripheral neuropathy in the rat? Pain **52:**233–242.
10. **Dev, K. K., K. Hofele, S. Barbieri, V. L. Buchman, and H. van der Putten.** 2003. α-Synuclein and its molecular pathophysiological role in neurodegenerative disease. Neuropharmacology **45:**14–44.
11. **Dickinson, T., R. Mitchell, P. Robberecht, and S. M. Fleetwood-Walker.** 1999. The role of VIP/PACAP receptor subtypes in spinal somatosensory processing in rats with an experimental peripheral mononeuropathy. Neuropharmacology **38:**167–180.
12. **Dickson, D. W.** 2001. Alpha-synuclein and the Lewy body disorders. Curr. Opin. Neurol. **14:**423–432.
13. **Eliezer, D., E. Kutluay, R. Bussell, Jr., and G. Browne.** 2001. Conformational properties of alpha-synuclein in its free and lipid-associated states. J. Mol. Biol. **307:**1061–1073.
14. **Filliatreau, G., N. Attal, R. Hassig, G. Guilbaud, J. Desmeules, and L. DiGiamberardino.** 1994. Time-course of nociceptive disorders induced by chronic loose ligatures of the rat sciatic nerve and changes of the acetylcholinesterase transport along the ligated nerve. Pain **59:**405–413.
15. **Galvin, J. E., B. Giasson, H. I. Hurtig, V. M. Lee, and J. Q. Trojanowski.** 2000. Neurodegeneration with brain iron accumulation, type 1 is characterized by alpha-, beta-, and gamma-synuclein neuropathology. Am. J. Pathol. **157:**361–368.
16. **Galvin, J. E., V. M. Lee, and J. Q. Trojanowski.** 2001. Synucleinopathies: clinical and pathological implications. Arch. Neurol. **58:**186–190.
17. **Galvin, J. E., K. Uryu, V. M. Lee, and J. Q. Trojanowski.** 1999. Axon pathology in Parkinson's disease and Lewy body dementia hippocampus contains alpha-, beta-, and gamma-synuclein. Proc. Natl. Acad. Sci. USA **96:**13450–13455.
18. **Giasson, B. I., J. E. Duda, M. S. Forman, V. M. Lee, and J. Q. Trojanowski.** 2001. Prominent perikaryal expression of alpha- and beta-synuclein in neurons of dorsal root ganglion and in medullary neurons. Exp. Neurol. **172:**354–362.
19. **Giasson, B. I., J. E. Duda, S. M. Quinn, B. Zhang, J. Q. Trojanowski, and V. M. Lee.** 2002. Neuronal alpha-synucleinopathy with severe movement disorder in mice expressing A53T human alpha-synuclein. Neuron **34:**521–533.
20. **Goedert, M.** 2001. Alpha-synuclein and neurodegenerative diseases. Nat. Rev. Neurosci. **2:**492–501.
21. **Guilbaud, G., M. Gautron, F. Jazat, H. Ratinahirana, R. Hassig, and J. J. Hauw.** 1993. Time course of degeneration and regeneration of myelinated nerve fibres following chronic loose ligatures of the rat sciatic nerve: can nerve lesions be linked to the abnormal pain-related behaviours? Pain **53:**147–158.
22. **Gundersen, H. J. G.** 1986. Stereology of arbitrary particles. A review of unbiased number and size estimators and the presentation of some new ones, in the memory of William R. Thompson. J. Microsc. **143:**3–45.
23. **Hashimoto, M., E. Rockenstein, M. Mante, M. Mallory, and E. Masliah.** 2001. Beta-synuclein inhibits alpha-synuclein aggregation. A possible role as an anti-parkinsonian factor. Neuron **32:**213–223.
24. **Jakes, R., M. G. Spillantini, and M. Goedert.** 1994. Identification of two distinct synucleins from human brain. FEBS Lett. **345:**27–32.
25. **Jensen, P. H., J. Y. Li, A. Dahlstrom, and C. G. Dotti.** 1999. Axonal transport of synucleins is mediated by all rate components. Eur. J. Neurosci. **11:**3369–3376.
26. **Ji, H., Y. E. Liu, T. Jia, M. Wang, J. Liu, G. Xiao, B. K. Joseph, C. Rosen, and Y. E. Shi.** 1997. Identification of a breast cancer-specific gene, BCSG1, by direct differential cDNA sequencing. Cancer Res. **57:**759–764.
27. **Konigsmark, B. W.** 1970. Methods for the counting of neurons, p. 315–340. *In* W. J. H. Nauta and S. O. E. Ebbesson (ed.), Contemporary research methods in neuroanatomy. Springer-Verlag, Berlin, Germany.
28. **Kruger, R., O. Eberhardt, O. Riess, and J. B. Schulz.** 2002. Parkinson's disease: one biochemical pathway to fit all genes? Trends Mol. Med. **8:**236–240.
29. **Lavedan, C., E. Leroy, A. Dehejia, S. Buchholtz, A. Dutra, R. L. Nissbaum, and M. H. Polymeropoulos.** 1998. Identification, localization and characterization of the human γ-synuclein gene. Hum. Genet. **103:**106–112.
30. **Lee, M. K., W. Stirling, Y. Xu, X. Xu, D. Qui, A. S. Mandir, T. M. Dawson, N. G. Copeland, N. A. Jenkins, and D. L. Price.** 2002. Human alpha-synuclein-harboring familial Parkinson's disease-linked Ala-53→Thr mutation causes neurodegenerative disease with alpha-synuclein aggregation in transgenic mice. Proc. Natl. Acad. Sci. USA **99:**8968–8973.
31. **Lesuisse, C., and L. J. Martin.** 2002. Long-term culture of mouse cortical neurons as a model for neuronal development, aging, and death. J. Neurobiol. **51:**9–23.
32. **Li, J.-Y., P. H. Jensen, and A. Dahlström.** 2002. Differential localization of α-, β- and γ-synucleins in the rat CNS. Neuroscience **113:**463–478.
33. **Lotharius, J., and P. Brundin.** 2002. Pathogenesis of Parkinson's disease: dopamine, vesicles and alpha-synuclein. Nat. Rev. Neurosci. **3:**932–942.
34. **McNaught, K. S., and C. W. Olanow.** 2003. Proteolytic stress: a unifying concept for the etiopathogenesis of Parkinson's disease. Ann. Neurol. **53:**S73-S84.
35. **Nakajo, S., K. Tsukada, K. Omata, Y. Nakamura, and K. Nakaya.** 1993. A new brain-specific 14-kDa protein is a phosphoprotein. Its complete amino acid sequence and evidence for phosphorylation. Eur. J. Biochem. **217:**1057–1063.
36. **Ninkina, N. N., M. V. Alimova-Kost, J. W. E. Paterson, L. Delaney, B. B. Cohen, S. Imreh, N. V. Gnuchev, A. M. Davies, and V. L. Buchman.** 1998. Organisation, expression and polymorphism of the human persyn gene. Hum. Mol. Genet. **7:**1417–1424.
37. **Ostrerova, N., L. Petrucelli, M. Farrer, N. Mehta, P. Choi, J. Hardy, and B. Wolozin.** 1999. Alpha-synuclein shares physical and functional homology with 14–3–3 proteins. J. Neurosci. **19:**5782–5791.
38. **Ostrerova-Golts, N., L. Petrucelli, J. Hardy, J. M. Lee, M. Farrer, and B. Wolozin.** 2000. The A53T alpha-synuclein mutation increases iron-dependent aggregation and toxicity. J. Neurosci. **20:**6048–6054.
39. **Pan, Z. Z., W. Bruening, B. I. Giasson, V. M. Lee, and A. K. Godwin.** 2002. Gamma-synuclein promotes cancer cell survival and inhibits stress- and chemotherapy drug-induced apoptosis by modulating MAPK pathways. J. Biol. Chem. **277:**35050–35060.
40. **Park, J. Y., and P. T. Lansbury, Jr.** 2003. Beta-synuclein inhibits formation of alpha-synuclein protofibrils: a possible therapeutic strategy against Parkinson's disease. Biochemistry **42:**3696–3700.
41. **Petrucelli, L., C. O'Farrell, P. J. Lockhart, M. Baptista, K. Kehoe, L. Vink, P. Choi, B. Wolozin, M. Farrer, J. Hardy, and M. R. Cookson.** 2002. Parkin protects against the toxicity associated with mutant alpha-synuclein: proteasome dysfunction selectively affects catecholaminergic neurons. Neuron **36:**1007–1019.
42. **Pinon, L. G., G. Middleton, and A. M. Davies.** 1997. Bcl-2 is required for cranial sensory neuron survival at defined stages of embryonic development. Development **124:**4173–4178.
43. **Rajagopalan, S., and J. K. Andersen.** 2001. Alpha synuclein aggregation: is it the toxic gain of function responsible for neurodegeneration in Parkinson's disease? Mech. Ageing Dev. **122:**1499–1510.
44. **Rockenstein, E., L. A. Hansen, M. Mallory, Q. Trojanowski, D. Galasko, and E. Masliah.** 2001. Altered expression of the synuclein family mRNA in Lewy body and Alzheimer's disease. Brain Res. **914:**48–56.
45. **Saha, A. R., N. N. Ninkina, D. P. Hanger, B. H. Anderton, A. M. Davies, and V. L. Buchman.** 2000. Induction of neuronal death by alpha-synuclein. Eur. J. Neurosci. **12:**3073–3077.
46. **Schluter, O. M., F. Fornai, M. G. Alessandri, S. Takamori, M. Geppert, R. Jahn, and T. C. Sudhof.** 2003. Role of alpha-synuclein in 1-methyl-4-phenyl-1,2,3,6-tetrahydropyridine-induced parkinsonism in mice. Neuroscience **118:**985–1002.
47. **Serpell, L. C., J. Berriman, R. Jakes, M. Goedert, and R. A. Crowther.** 2000.

Fiber diffraction of synthetic alpha-synuclein filaments shows amyloid-like cross-beta conformation. Proc. Natl. Acad. Sci. USA **97:**4897–4902.

48. **Specht, C. G., and R. Schoepfer.** 2001. Deletion of the alpha-synuclein locus in a subpopulation of C57BL/6J inbred mice. BMC Neurosci. **2:**11. [Online.] http://www.pubmedcentral.gov/articlerender.fcgi?tool=pubmed&pubmedid=11591219.
49. **Suzuki, K., E. Iseki, O. Katsuse, A. Yamaguchi, K. Katsuyama, I. Aoki, S. Yamanaka, and K. Kosaka.** 2003. Neuronal accumulation of alpha- and beta-synucleins in the brain of a GM2 gangliosidosis mouse model. Neuroreport **14:**551–554.
50. **Tabrizi, S. J., M. Orth, J. M. Wilkinson, J. W. Taanman, T. T. Warner, J. M. Cooper, and A. H. Schapira.** 2000. Expression of mutant alpha-synuclein causes increased susceptibility to dopamine toxicity. Hum. Mol. Genet. **9:**2683–2689.
51. **Tanaka, Y., S. Engelender, S. Igarashi, R. K. Rao, T. Wanner, R. E. Tanzi, A. L. Sawa, V. Dawson, T. M. Dawson, and C. A. Ross.** 2001. Inducible expression of mutant alpha-synuclein decreases proteasome activity and increases sensitivity to mitochondria-dependent apoptosis. Hum. Mol. Genet. **10:**919–926.
52. **Tiunova, A. A., K. V. Anokhin, A. R. Saha, O. Schmidt, D. P. Hanger, B. H. Anderton, A. M. Davies, N. N. Ninkina, and V. L. Buchman.** 2000. Chicken synucleins: cloning and expression in the developing embryo. Mech. Dev. **99:**195–198.
53. **Trojanowski, J. Q., and V. M. Lee.** 2002. Parkinson's disease and related synucleinopathies are a new class of nervous system amyloidoses. Neurotoxicology **23:**457–460.
54. **Tybulewicz, V. L., C. E. Crawford, P. K. Jackson, R. T. Bronson, and R. C. Mulligan.** 1991. Neonatal lethality and lymphopenia in mice with a homozygous disruption of the c-abl proto-oncogene. Cell **65:**1153–1163.
55. **Uversky, V. N., J. Li, P. Souillac, I. S. Millett, S. Doniach, R. Jakes, M. Goedert, and A. L. Fink.** 2002. Biophysical properties of the synucleins and their propensities to fibrillate. Inhibition of alpha-synuclein assembly by beta- and gamma-synucleins. J. Biol. Chem. **277:**11970–11978.
56. **van der Putten, H., K. H. Wiederhold, A. Probst, S. Barbieri, C. Mistl, S. Danner, S. Kauffmann, K. Hofele, W. P. Spooren, M. A. Ruegg, S. Lin, P. Caroni, B. Sommer, M. Tolnay, and G. Bilbe.** 2000. Neuropathology in mice expressing human alpha-synuclein. J. Neurosci. **20:**6021–6029.
57. **Wallace, V. C., D. F. Cottrell, P. J. Brophy, and S. M. Fleetwood-Walker.** 2003. Focal lysolecithin-induced demyelination of peripheral afferents results in neuropathic pain behavior that is attenuated by cannabinoids. J. Neurosci. **23:**3221–3233.
58. **Woolf, C., and S. Thompson.** 1991. The induction and maintenance of central sensitization is dependent on N-methyl-D-aspartic acid receptor activation–implications for the treatment of postinjury pain hypersensitivity states. Pain **44:**293–299.